The Pennsylvania State University

The Graduate School

Department of Mechanical Engineering

AN INVESTIGATION INTO COMPUTER SIMULATION OF THE DYNAMIC RESPONSE OF A GAS TURBINE ENGINE

A Paper in

Mechanical Engineering

by

Todd B. Henricks, P. E.
Lieutenant, Civil Engineer Corps
United States Navy

Submitted in Partial Fulfillment
of the Requirements
for the Degree of

Master of Science

July 1997

ABSTRACT

Transient performance of gas turbines has a strong bearing on output and component life. For this reason, several articles have been written on the dynamic simulation of gas turbine systems in electrical generation, cogeneration, and marine applications. These models provide a basis for this present work. This paper describes a mathematical and computer model that was developed to investigate the dynamic response of a simple (no reheat, regeneration, or other auxiliary equipment) single-shaft gas turbine system. The model uses design parameters normally incorporated in gas turbine design (e.g. load coefficient, flow coefficient, and deHaller Number) as well as compressor and turbine stage geometry and compressor and turbine material properties. Also incorporated is a combustion chamber model. Other input parameters are included to enable the model to be adaptable to various system sizes and environments.

The results of several trials are displayed, showing how given parameters (e.g. fuel-air ratio, load, and efficiencies) were varied and results were compared. A thermodynamic balance resulted in a 26% system thermal efficiency for the reference state parameters. Also, a start-up procedure similar to an industrial gas turbine system was simulated with this model.

Examination of the results from the trial runs show the computer model to be reliable, given that no control system was incorporated. Because of the approach used, the computer model is easily adaptable to further improvements and a control system.

TABLE OF CONTENTS

NOMENCLATURE

B	Hub-to-Tip Ratio
cbh	Compressor Blade Height (m)
cdr	Compressor Disk Radius (m)
C_p	Specific Heat (J/kg K)
f	Fuel-to-Air Ratio
H	deHaller Number
h	Enthalpy (J/kg)
I	Moment of Inertia (kg m^2)
k	Ratio of Specific Heats
$\dot{m}$	Mass Flow Rate (kg/s)
P	Pressure (Pa)
$\dot{P}$	Power (kW)
r	Radius
R	Degree of Reaction
T	Temperature (K)
U	Blade Tip Speed (m/s)
V	Velocity (m/s)
W	Work (J/kg)

Greek Symbols

η	Efficiency
ρ	Density of Air (kg/m^3)
τ	Torque (N m)
ϕ	Flow Coefficient
ψ	Load Coefficient
Ω	Angular Velocity (rad/sec)
$\dot{\Omega}$	Angular Acceleration (rad/sec^2)

Subscripts

a	Axial
C	Compressor
L	Load
mix	Combustion mixture (fuel and air)
r	Root
S	Stage
t	Tip
T	Turbine
0	Stagnation
1	Compressor Inlet
2	Compressor Outlet
3	Turbine Inlet
4	Turbine Outlet

ACKNOWLEDGEMENTS

I would like to express deep appreciation to the following people and organizations for their help and support during this past year:

To the United States Navy, for giving me this opportunity to attend The Pennsylvania State University.

To Mr. Jack McGroarty and the Naval Surface Warfare Center, Naval Ships Systems Engineering Station - Carderock Division, Philadelphia, Pennsylvania, for his enthusiasm for the project and supporting me with the software to build this computer model.

To Dr. Horacio Perez-Blanco, for being my advisor, mentor, and friend through this very short, and busy, year. Thank you for understanding my unique situation and helping me accomplish this degree.

To Dr. Gita Talmage, for your encouragement and words of wisdom every time I felt the pressure mounting.

To Jim Roche, Matt Stoner, and Mike Moeney, for your friendship, patience, and help during this past year.

To my Mom and Dad, for your unfailing support and trust that encouraged me throughout these many years.

And finally, to my loving wife, Tammy. Without you I could not have accomplished this. Your prayers, support, understanding, patience, and love are what made this possible. Thank you with all of my heart.

Romans 10:9 (KJV) That if thou shalt confess with thy mouth the Lord Jesus, and shalt believe in thine heart that God hath raised him from the dead, thou shalt be saved.

Romans 10:13 (KJV) For whosoever shall call upon the name of the Lord shall be saved.

INTRODUCTION

Transient performance of gas turbines has a strong bearing on output and component life. Issues of thermal fatigue [1] can influence the start-up sequence, since rapid start-ups can impair turbine blade life. As hot gas is generated in the combustion chamber from a cold-start, gradual (as opposed to sudden) heating of the turbine components reduces thermal stresses associated with the start-up. Consequently, the turbine is activated by external power with air inlet guide vanes (IGVs) closed, while the combustion chamber is simply in a heating duty for about ten minutes. Synchronization with the electrical load in the case of power generation also requires accurate speed control under varying load.

In marine propulsion applications, system response in terms of fuel consumption for an oscillatory load is also of concern [2]. Different control strategies were analyzed in this work, namely Proportional Integral and Linear Quadratic Regulator. Both were shown to offer strengths and drawbacks with regards to operational aspects. This work shows the great value that dynamic modeling can offer in terms of system evaluation prior to actual construction. Inevitably, the conclusions depend on the model adopted for the gas turbine, as described in [3]. The model used here for the gas turbine has a definitive empirical slant, since it is largely based on

performance data and time lags acquired from an actual gas turbine test bed. This approach was expanded and refined in [4].

Rather complex systems have been modeled based on similar empirical approaches [5]. In this case, a cogeneration plant consisting of a gas turbine, a boiler, and two steam turbines (high and low pressure), were simulated. The system was approximated by using the performance curves given by manufacturers, and adding necessary time lags based on manufacturer information. Time-dependent equations were integrated with Euler's method. It was concluded that dynamic simulation was a valuable tool for assessing the suitability of controls and safety measures.

A more basic approach to modeling was adopted in [6]. The basic thermodynamic equations for mass and energy balances were used for model formulation, as opposed to manufacturer's curves. Yet, the inertia of rotors and shafts was absent from the equations, which probably explains the need found by the authors to add time lags to this model. The model effectively predicted behavior during load perturbations at full load. A slightly more recent work focused on developing the gas turbine model based on design parameters [7]. Load coefficients and stage efficiencies were employed for this simulation, along with part-load losses extracted from the literature. Again, inertial aspects seem to have been neglected by the author.

The need to combine basic thermodynamic equations with inertial aspects for generic models was recognized recently. In [8], the transient equations for inlet duct pressure and mass flow rate were formulated. Compressor and combustion chamber conditions were calculated from a transient analysis coupled with polytropic process equations. The thermal inertia of all components was neglected, and performance maps of each component were used to obtain isentropic efficiencies. A dynamic equilibrium equation was used to calculate the acceleration of the turbine. Good comparisons with experimental performance were obtained.

The present work is inserted in this context: whereas most models are semiempirical, in that they rely on time constants and performance maps, serious recent attempts to extend the generality of gas turbine models have been made. Clearly, the flexibility of a model to competently handle a wide variety of turbines is the target. Similar to previous work, the trend of formulating the basic mechanical and thermal equations for each component is followed here. In an extension of previous work, it is attempted wherever possible to include mechanical and thermal design parameters to broaden the reach of the model. Here, the main contribution consists of modeling the compressor stage by stage, and of including thermal and mechanical inertial effects based on first-principles, rather than empirical constants.

It is realized that complex machines cannot always be represented by simple models. Hence, the limitations of this approach are clear, especially at part-load. However, with the advent of computing power and of transient simulation software, it is inefficient to restrict modeling to numerical fitting of performance curves. Based on a literature search and this present work, it is ascertained that models of this type will be used more and more in the future to establish feasibility of design and of control and operating strategies.

DEVELOPMENT OF THE MATH MODEL

The mathematical model of the turbine system is based upon the three main components as seen in Figure 1 below: compressor, combustion chamber, and turbine. In addition to these main components, there is a component of mass flow rate included in the model.

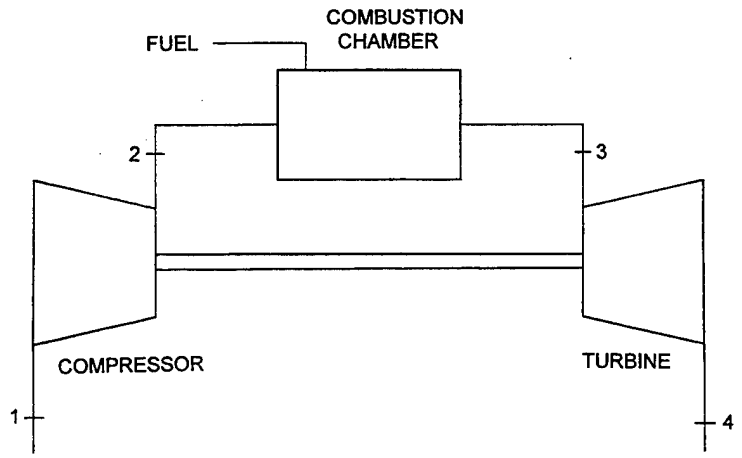

Figure 1. Schematic of the three main components: compressor, combustion chamber, and turbine.

Assumptions

These assumptions are used in the development of the gas turbine model:

(1) For the purposes of inertial calculations, compressor and turbine stages can be modeled as disks with rectangular blades attached on the edge of the disk.

(2) The increase in size of each successive stage of the compressor and the decrease in size of each successive stage of the turbine are approximated by constant factors.

(3) Rotors in the compressor and turbine are perfectly balanced.

(4) The compression and expansion processes are adiabatic.

(5) Air acts as an ideal gas.

(6) The compressor inlet pressure is equal to the turbine outlet pressure.

(7) There are 16 compressor stages and 4 turbine stages.

(8) Stage efficiencies for the compressor and turbine are constant.

(9) The combustors can be modeled as open-ended cylinders of constant wall thickness.

(10) The temperature drop across the turbine is divided equally among the four stages. This distribution may be altered as desired.

The turbine and compressor, along with the load, are connected to a single shaft, such that the dynamic equation of the shaft is:

$$\tau_T = \tau_C + \tau_L + f_L + \left(I_C \cdot \dot{\Omega}\right) + \left(I_T \cdot \dot{\Omega}\right) \qquad (1)$$

Each component of the model is described below.

Compressor and Turbine Stages

To model the moments of inertia of the rotating masses in the compressor and the turbine, each stage is modeled as a disk with rectangular blades attached as seen in Figure 2a:

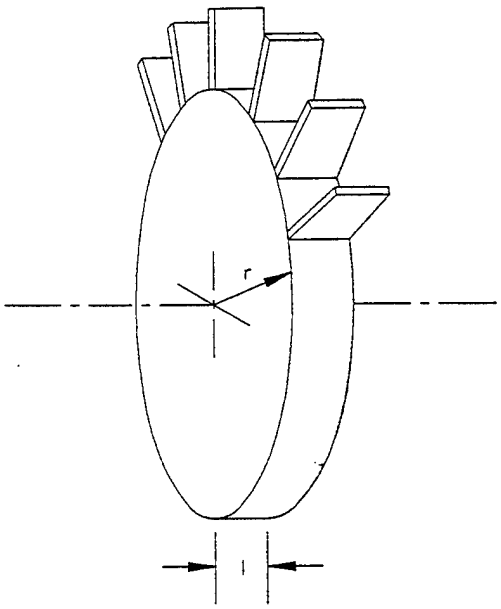

Figure 2a. Model of compressor and turbine stage.

This moment of inertia model is derived from the model of a rotating disk found in reference [9]. Although the cross-sectional free area is a function of the design flow rate and blockage coefficients, a simpler approach was used to model the radial dimensions. First, a cross-section of the stage radius was assumed, as seen in Figure 2b. The dimensions shown are relative to the

design radius of the stage (r). Each of the cross-hatched areas was modeled as a rotating ring, and the section at the center line was modeled as a rotating disk. These sections were added for the total moment of inertia for one stage, and then modeled as a single rotating disk, as previously seen in Figure 2a. The blades were then added into the moment of inertia calculation.

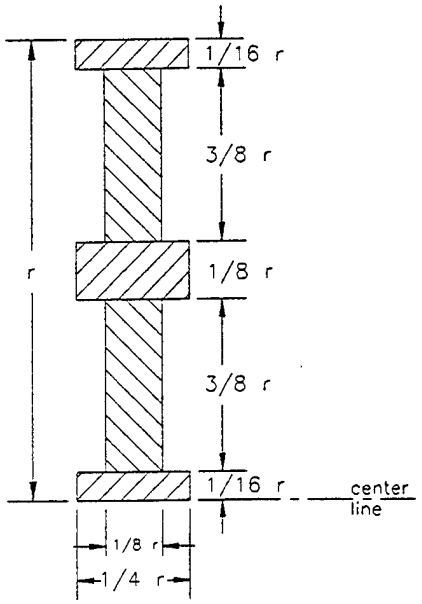

Figure 2b. Cross-section of a compressor and turbine stage.

For each successive stage in the compressor (decreasing in size) and each successive stage in the turbine (increasing in size), a constant "decrease factor" (compressor) and "increase factor" (turbine) was used to estimate the

change in size (see Figures 3a and 3b below). The mass of all 16 compressor stages were summed for a total mass, and the same was done for the 4 turbine stages. Using these parameters, the total moment of inertia was calculated for the compressor (I_C) and the turbine (I_T).

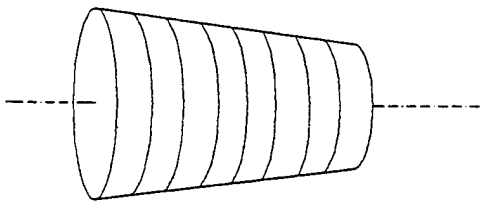

Figure 3a. The compressor is modeled as a series of 16 approximately linearly decreasing stage sizes.

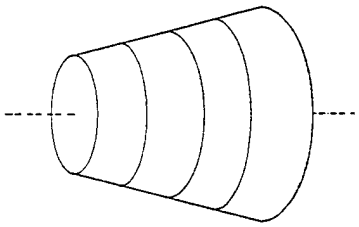

Figure 3b. The turbine is modeled as a series of 4 approximately linearly increasing stage sizes.

Compressor

The model of this component is based upon the specification of design variables normally employed to characterize a given turbine design. Hence, the compressor model was developed using load coefficient, deHaller Number, flow coefficient, degree of reaction, and stage geometry. Starting with degree of reaction and load coefficient, the equations used are [10]:

$$\psi = \frac{(h_{02} - h_{01})}{U^2} \tag{2}$$

$$R = \frac{C_p(T_2 - T_1)}{h_{02} - h_{01}} \tag{3}$$

and for the blade tip speed, U,

$$U = (\text{radius} + \text{blade\_ height}) \cdot \Omega \tag{4}$$

Combining equations (2), (3) and (4), the temperature rise in each compressor stage can be calculated as follows:

$$T_{02S} = T_{01S} + \frac{(cdr + cbh)^2 \cdot \psi \cdot \Omega^2}{\eta_{CS} \cdot C_p} \tag{5}$$

where "cdr" is the compressor disk radius and "cbh" is the compressor blade height.

Successively using equation (5) for each stage results in the compressor exit temperature. The pressure rise in each stage is found by using the following equation:

$$P_{2S} = P_{1S} \cdot \left(\frac{T_{02S}}{T_{01S}}\right)^{\frac{\eta_{cs} \cdot k}{k-1}} \tag{6}$$

The compressor isentropic efficiency, η_C, is found using the relationship between polytropic and isentropic efficiencies [11]:

$$\eta_c = \frac{\left(\frac{P_2}{P_1}\right)^{\frac{(k-1)}{k}} - 1}{\left(\frac{P_2}{P_1}\right)^{\frac{(k-1)}{k \cdot \eta_{cs}}} - 1} \tag{7}$$

The torque required by the compressor is found by again using degree of reaction, deHaller Number, load coefficient, flow coefficient, and stage blade tip speed:

$$R = \frac{h_2 - h_1}{h_{02} - h_{01}} \tag{8}$$

where $(h_{02} - h_{01})$ is:

$$h_{02} - h_{01} = \left(h_2 + \frac{V_2^2}{2}\right) - \left(h_1 + \frac{V_1^2}{2}\right) \tag{9}$$

Combining equations (8) and (9) and letting

$$h_{02} - h_{01} = \Delta h_0$$

results in

$$R = \frac{\Delta h_0 - \frac{1}{2} \cdot V_1^2 \cdot \left(\frac{V_2^2}{V_1^2} - 1 \right)}{\Delta h_0}$$

Substituting in the deHaller number, H,

$$H = \frac{V_2}{V_1} \tag{10}$$

results in

$$R = 1 + \frac{\frac{1}{2} \cdot V_1^2 \cdot \left(1 - H^2\right)}{\Delta h_0} \tag{11}$$

Definitions of Flow coefficient and Load coefficient are:

$$\phi = \frac{V}{U} \tag{12}$$

$$\psi = \frac{\Delta h_0}{U^2} \tag{13}$$

Taking equations (12) and (13), and substituting them into equation (11) results in a relationship between degree of reaction, load coefficient, and flow coefficient:

$$R = 1 + \frac{\frac{1}{2} \cdot \phi^2 \cdot \left(1 - H^2\right)}{\psi} \tag{14}$$

The difference in stagnation enthalpies is the stage work [10],

$$\Delta h_0 = 2 \cdot U \cdot \left(V_{u1} - V_{u2}\right) = W_S \tag{15}$$

and combining this with the load coefficient defined as [10]:

$$\psi = \frac{C_P \cdot \Delta T_0}{2 \cdot U^2} \tag{16}$$

results in

$$\psi = \frac{W_S}{U^2} \tag{17}$$

Using two definitions of power,

$$\dot{P} = \Omega \cdot \tau_S \qquad \text{and} \qquad \dot{P} = \dot{m} \cdot W_S$$

equating and solving for the stage work, W_S, results in:

$$W_S = \frac{\Omega \cdot \tau_S}{\dot{m}}$$

Combining this with equation (17),

$$\psi = \frac{\Omega \cdot \tau_S}{U^2 \cdot \dot{m}} \tag{18}$$

Equating equations (16) and (18),

$$\frac{C_P \cdot \Delta T_{0S}}{2 \cdot U^2} = \frac{\Omega \cdot \tau_S}{U^2 \cdot \dot{m}}$$

The stage torque can be found as

$$\tau_S = \frac{m \cdot C_P \cdot \left(T_{02} - T_{01}\right)_S}{\Omega} \tag{19}$$

Additionally, the compressor efficiency must be taken into account. Recalling the load coefficient, equation (13),

$$\psi = \frac{\Delta h_0}{U^2} \qquad \text{(ideal)}$$

$$\psi = \frac{\Delta h_0 \cdot \eta_c}{U^2} \qquad \text{(actual)}$$

Using this efficiency, and the fact that the temperature differences are summed across all the stages, the total compressor torque can be calculated as follows:

$$\tau_C = \frac{\dot{m} \cdot C_P \cdot (T_{02} - T_{01})}{\Omega \cdot \eta_C} \qquad (20)$$

Turbine

The torque imparted from the fluid onto the turbine is developed starting with the work of an individual stage of the turbine:

$$W_S = C_{pmix} \cdot \left(T_3 - T_4\right)_S \tag{21}$$

Substituting this into the load coefficient definition [10]:

$$\psi = -\left(\frac{2 \cdot W_S}{U^2}\right) \tag{22}$$

and from equation (4),

$$U = (tdr + tbh) \cdot \Omega \tag{23}$$

where "tdr" is the turbine disk radius and "tbh" is the turbine blade height.

Substituting equation (23) into equation (22),

$$\psi = -\frac{2 \cdot W_S}{(tdr + tbh)^2 \cdot \Omega^2} \tag{24}$$

Again using the definitions of power,

$$\dot{P} = \Omega \cdot \tau_S \qquad \text{and} \qquad \dot{P} = \dot{m} \cdot W_S$$

and solving for τ_S:

$$\tau_S = \frac{W_S \cdot \dot{m}}{\Omega}$$

Using the fact that the mass flow rate through the turbine is the mass flow rate of air plus the mass flow rate of fuel, so the stage torque becomes

$$\tau_S = \frac{W_S \cdot (1 + f) \cdot \dot{m}}{\Omega} \qquad (25)$$

The turbine efficiency is factored into the above expression as follows:

$$\psi = \frac{\Delta h_0}{U^2} \qquad \text{(ideal)}$$

$$\psi = \frac{\Delta h_0}{U^2 \cdot \eta_T} \qquad \text{(actual)}$$

Where the turbine efficiency is found using the relationship between polytropic and isentropic efficiencies [11]:

$$\eta_T = \frac{1 - \left(\frac{P_4}{P_3}\right)^{\frac{(k-1)\cdot\eta_{TS}}{k}}}{1 - \left(\frac{P_4}{P_3}\right)^{\frac{(k-1)}{k}}} \qquad (26)$$

In addition, the turbine outlet temperature is calculated and knowing the ambient pressure and turbine inlet temperature as follows:

$$T_4 = T_3 \cdot \left(\frac{P_4}{P_3}\right)^{\left(\frac{(k-1)\cdot\eta_T}{k}\right)} \tag{27}$$

Substituting equation (21) into equation (25) and incorporating the efficiency results in the turbine torque equation:

$$\tau_T = \frac{\dot{m} \cdot (1 + f) \cdot C_{Pmix} \cdot (T_3 - T_4) \cdot \eta_T}{\Omega} \tag{28}$$

The load coefficient of the turbine is calculated using the temperature drop across the turbine as a parameter:

$$\Delta T_S = \frac{T_3 - T_4}{4} \tag{29}$$

$$\psi_T = \frac{C_p(\Delta T_S)}{2 \cdot (tdr + tbh)^2 \cdot \Omega^2 \cdot \eta_T} \tag{30}$$

Mass Flow Rate

An equation for mass flow rate through the compressor is given by [11]:

$$\dot{m} = \rho \cdot A \cdot V = \rho \cdot \pi \cdot r_t^2 \cdot \left[1 - \left(\frac{r_r}{r_t}\right)^2\right] \cdot V_a \qquad (31)$$

Making the following substitutions into equation (31)

$$r_t = cdr + cbh$$

$$B = \frac{r_r}{r_t}$$

$$V_a = \phi \cdot \Omega$$

the mass flow rate can be calculated as follows:

$$\dot{m} = \rho \cdot \pi \cdot (cdr + cbh)^2 \cdot \left(1 - B^2\right) \cdot \phi \cdot \Omega \qquad (32)$$

where the density is calculated using the ideal gas law.

Combustion Chamber

The model for the combustion chamber is developed using the thermal mass of the chamber itself, the thermal mass of the fuel-air mixture, and the thermal mass of the first stage of the turbine. A control volume analysis of the combustion chamber reveals the following differential equation:

$$\left(\dot{m}_2\right) \cdot \left[C_P \cdot T_{02}\right] + \left(\dot{m}_f\right) \cdot (LHV)$$

$$= \left(\dot{m}_3\right) \cdot \left[C_P \cdot T_{03}\right] + \left(mC_P\right) \cdot \dot{T}_{03} \qquad (33)$$

where mC_P is the thermal mass of the system, which is modeled as follows:

$$mC_P = \left[\rho \cdot C_P \cdot Vol\right]_{can} + \left[\rho \cdot C_P \cdot Vol\right]_{\substack{fuel-air \\ mixture}} + \left[\rho \cdot C_P \cdot Vol\right]_{\substack{first \\ turbine \\ stage}} \qquad (34)$$

The pressure drop across the combustion chamber is calculated by:

$$P_3 = P_1 + \left(1 - \beta\right) \cdot \left(P_2 - P_1\right) \qquad (35)$$

where "β" is the fractional pressure drop across the combustion chamber.

The complete mathematical model is comprised of equation (1) as the basic equation, using equation (20) for τ_C, equation (28) for τ_T, calculated values for I_C and I_T, and user-input load and friction torques. The independent variable in these equations is time (t). The remaining equations in the mathematical model are:

mass flow rate .....(32)
compressor outlet temperature .....(5)
compressor outlet pressure.....(6)
compressor isentropic efficiency.....(7)
turbine isentropic efficiency .....(26)
turbine outlet temperature.....(27)
turbine load coefficient.....(30)
turbine inlet temperature ..... (33) and (34)
combustion chamber pressure drop.....(35)

DEVELOPMENT OF THE COMPUTER MODEL

Similar work has been done in simulating gas turbine systems. References [3] and [4] describe a linear model, while [8] describes a non-linear model similar to this paper. However, this model provides inputs for compressor and turbine stage geometry and design parameters such as B (hub-to-tip ratio), ψ (load coefficient), and ϕ (flow coefficient). Additionally, this program integrates a combustion chamber model. Several other inputs are required to run the model, including ambient conditions, compressor and turbine efficiencies, and compressor and turbine material properties. These input parameters enable this model to be adapted to a wide variety of gas turbine systems and environments. It is important to note that this model does not incorporate a control system as in [2] and [12]. However, the model is easily adaptable to such a system.

The software package VisSim ® was chosen for this model because it provides "a visual environment for developing continuous, discrete, multirate, and hybrid system models and performing dynamic simulations [13]." There are several other special features about VisSim ® outlined in [13] that make this a superb platform. The program itself is called "gtsim1.vsm" created by the author.

Figure 4 is the "top level" of gtsim1.vsm which shows the basic logic and interconnections of the previously discussed mathematical model. The program incorporates equation (1) as the basic equation, using equation (20) for τ_C, equation (28) for τ_T, calculated values for I_C and I_T, and input load and friction torques. The load and friction torques are computed as constant factors multiplied by the square of the angular velocity $[sec^{-1}]^2$.

Additionally, gtsim1.vsm uses the following equations for the associated parameters:

mass flow rate ..... (32)
compressor outlet temperature ..... (5)
compressor outlet pressure ..... (6)
compressor isentropic efficiency ..... (7)
turbine isentropic efficiency ..... (26)
turbine outlet temperature ..... (27)
turbine load coefficient ..... (30)
turbine inlet temperature ..... (33) and (34)
combustion chamber pressure drop ..... (35)

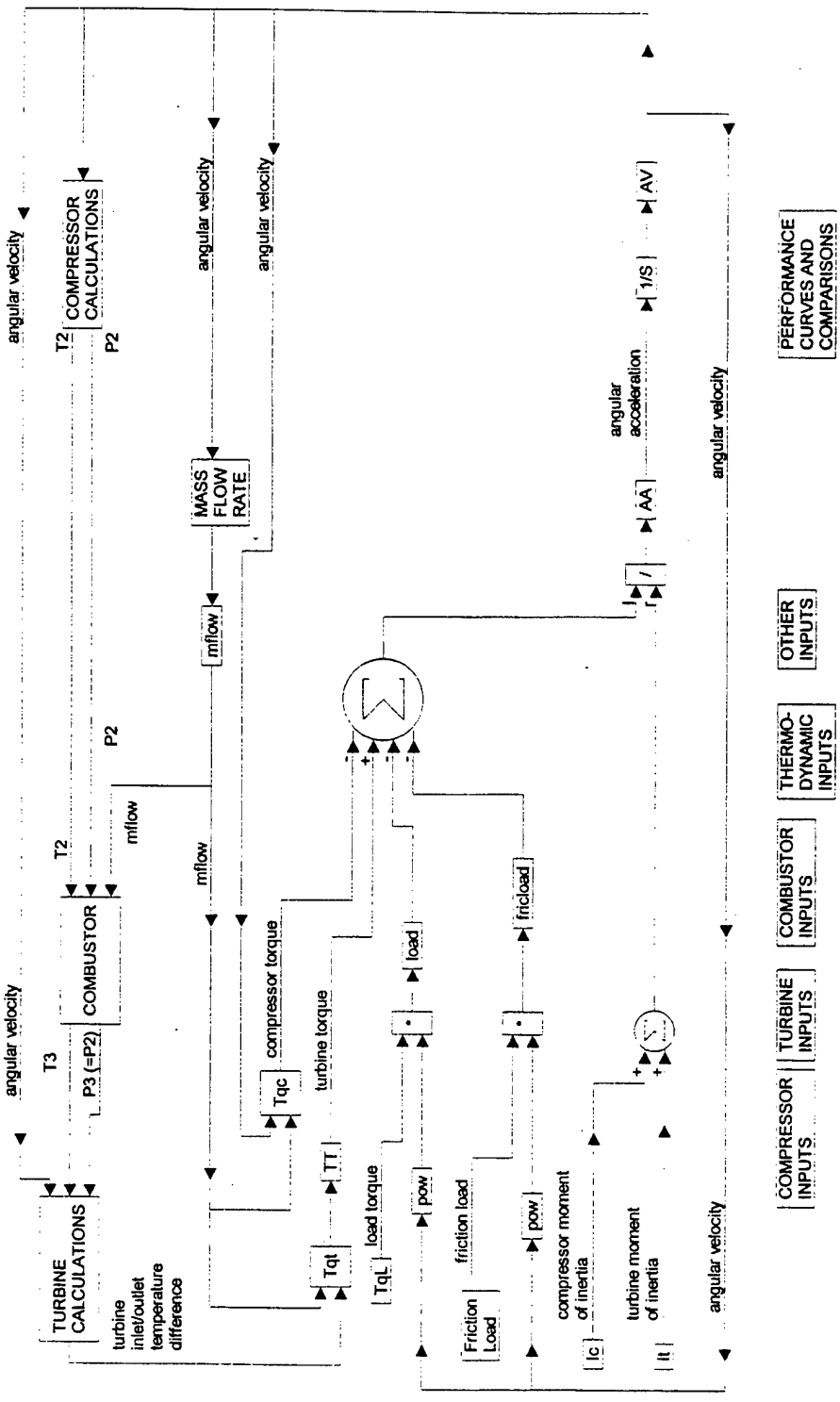

Figure 4. Top level of gtsim1.vsm, showing the basic logic of the program. Arrowheads indicate the direction of "signals" being processed.

RESULTS

To demonstrate the versatility of this model, several parameters were varied independently. In each case, all variables were held to their reference state (Appendix A) except the variable under discussion.

Reference State Run

Figure 5 shows the adopted baseline run. This run is based on a start-up from "cold" conditions, at constant fuel/air ratio, with a frictional load proportional to the square of the rotational velocity. Note that in this plot, the angular velocity is left in units of [s^{-1}] in order to clearly fit into the plot scale. The model allows an understanding of the variables in the uncontrolled start-up scenario. As long as the turbine produces no work, T_3 (peak cycle temperature) and T_4 (discharge temperature) are quite close. The compressor discharge pressure increases gradually with time. The air-breathing nature of this turbomachine is clearly reflected here: as soon as the speed increases and the air mass flow ramps up, compressor pressure and peak temperature start to increase sharply. As both T_3 and P_2 increase toward the design value, the turbine power output also increases.

Congruently, T_4 decreases, and the mass flow rate rapidly increases towards its design value. At steady-state conditions, the turbine develops 56.6 MW to drive the load.

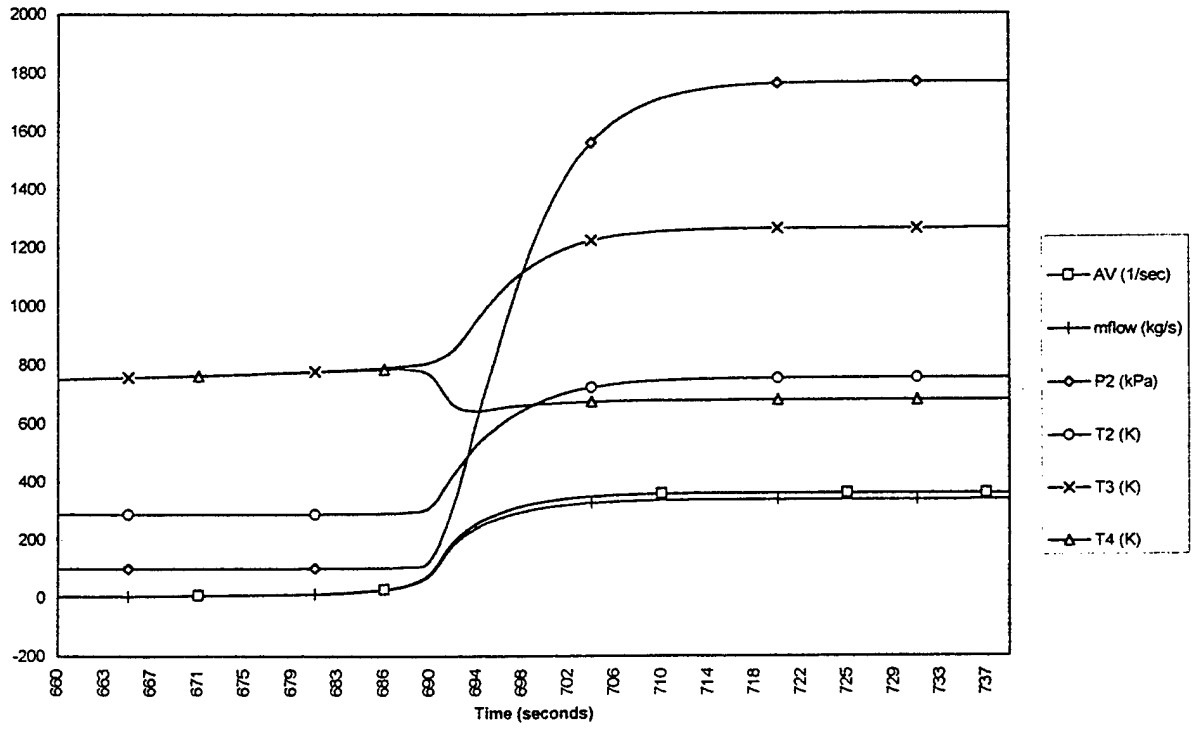

Figure 5. Response of turbine to baseline conditions (fuel/air ratio = 0.013, standard atmospheric conditions, and friction load and shaft load proportional to angular velocity squared). Start-up is from "cold" conditions at constant fuel/air ratio with frictional load. Inlet guide vanes (IGVs) are completely open.

Energy Balance

A control-volume energy balance was performed on each component of the model to ensure realistic parameters were passed between components and realistic output power values were obtained. Table 1 below gives values for this analysis. For this system at the adopted baseline parameters (Appendix A), the overall thermal efficiency was found to be 26%.

Component	Power Out (MW)	Component	Power In (MW)
Compressor	158.8	Compressor	158.8
Friction	5.19	Air	98.37
Exhaust	256.8	Fuel	220.2
Load	56.58		
Total	477.7	**Total**	477.7

Table 1. Thermodynamic balance of the adopted baseline run.

Start-Up Runs

In the following figures and tables, a given parameter was varied and the system allowed to start up from initial conditions. The resulting steady-state speed and time to reach the steady-state speed for each case is shown.

In Figure 6, the fuel-air ratio (held constant from turbine start-up to steady-state) was varied with the same start-up rotational velocity of 30 RPM. Up to approximately 500 seconds, the speed is the same for all three cases (f/a = 0.012, f/a = 0.013, and f/a = 0.014). After approximately 500 seconds, it is seen that for greater fuel-to-air ratios, less time is needed to reach higher steady-state speeds.

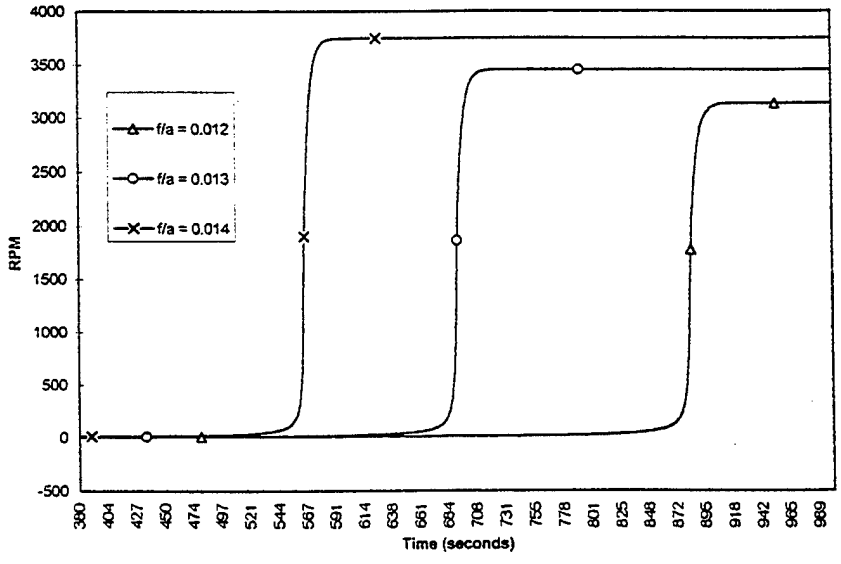

Figure 6. Influence of fuel to air ratio on response time and final velocity.

Figure 7 demonstrates the effect of compressor polytropic (small stage) efficiency [11] on steady-state speed. The plot shows that the rotational speed of the system increases as the compressor polytropic efficiency increases. This is due to the ability of a more efficient compressor to impart more work to a given amount of air. The greater work results in increased peak pressure, which in turn increases turbine output.

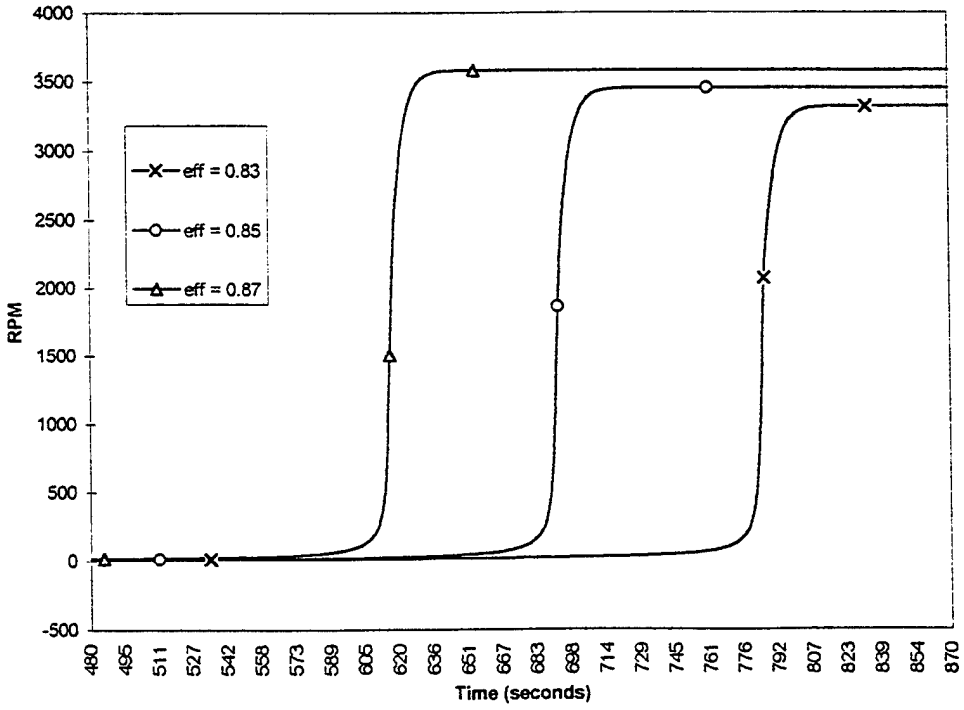

Figure 7. Influence of compressor polytropic efficiency on response time and rotational velocity .

Figure 8 demonstrates the effect of turbine polytropic (small stage) efficiency [11] on steady-state speed. The plot shows that as the turbine polytropic efficiency increases, the rotational speed of the system increases. This is due to the ability of a more efficient turbine to take more work from the combustion gases and use it to drive the compressor, friction load, and shaft load.

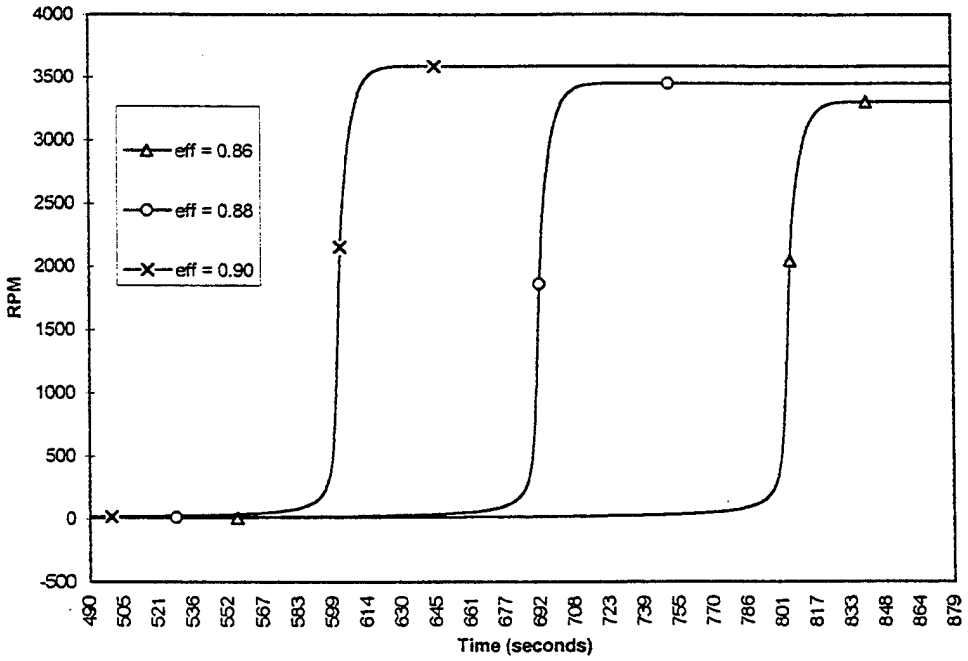

Figure 8. Influence of turbine polytropic efficiency on response time and rotational velocity.

Tables 2 and 3 below demonstrate the results of varying compressor load coefficient (ψ) and compressor blade height, respectively. Here in Table 2, increasing the load coefficient means that more work is communicated per stage to the air. Hence, the peak pressure increases, resulting in a more efficient cycle which leads to greater power output.

Load Coefficient ψ	Steady-State RPM	Time (sec) to Steady-State RPM
0.25	3296	925
0.30	3450	725
0.35	3536	615

Table 2. The effect of varying compressor load coefficient (ψ) (the ratio of stage work to blade kinetic energy). As the load coefficient is increased, the final speed also increases. This is due to the increased amount of work per stage as speed increases.

In Table 3 below, it is seen that the model responds reasonably as the blade height is increased. The longer blades can sweep more air at a given rotational velocity, resulting in increased power output.

Compressor Blade Height (m)	Steady-State RPM	Time (sec) to Steady-State RPM
0.39	3256	950
0.41	3450	725
0.43	3629	575

Table 3. The effect of varying compressor blade height. As the blade height is increased, there is more "swept" area through which more mass can flow during a revolution of the compressor stage. The direct result is that for more mass flow, more power, and hence, greater steady-state speed.

Variations During Steady-State Operation

For these runs, the model was allowed to ramp-up to its reference steady-state conditions from a "cold" start. The amount of time taken to get to these reference conditions was approximately 725 seconds. From the steady-state conditions, certain parameters were varied as described below and results compared.

Figure 9 shows the effect of load changes during steady-state operation of the gas turbine. "Load - Decreased" indicates that the constant load factor (the factor multiplied by the square of the angular velocity to obtain the actual load) was instantaneously reduced from 1.2 to 1.0. "Load - constant" indicates no change in the load, and "Load - Increased" indicates that the constant factor was instantaneously increased from 1.2 to 1.4. The load was decreased and increased at different times for clarity. The results are as expected: an increased load results in lower rotational speed and a decreased load results in higher rotational speed.

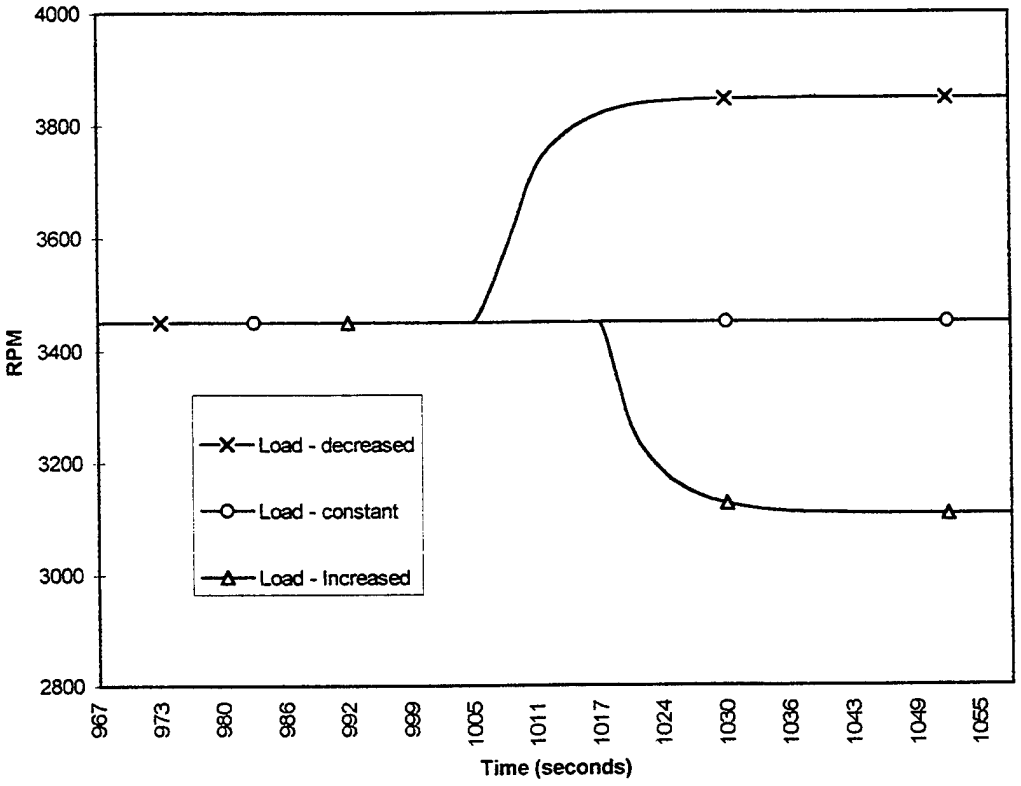

Figure 9. Influence of changes in load during steady-state operations.

Figure 10 is similar to Figure 9, except that the fuel-air ratio instead of the load is changed during steady-state operations. In Figure 10, "f/a decreased" indicates that the fuel-air ratio was decreased from 0.013 to 0.012, "f/a constant" indicates no change, and "f/a increased indicates that the fuel-air ratio was increased from 0.013 to 0.014. Again, the parameter (fuel-air ratio) was decreased and increased at slightly different times for clarity. The results are again as expected: increased fuel-air ratio results in higher rotational speed and a decreased fuel-air ratio results in lower rotational speed.

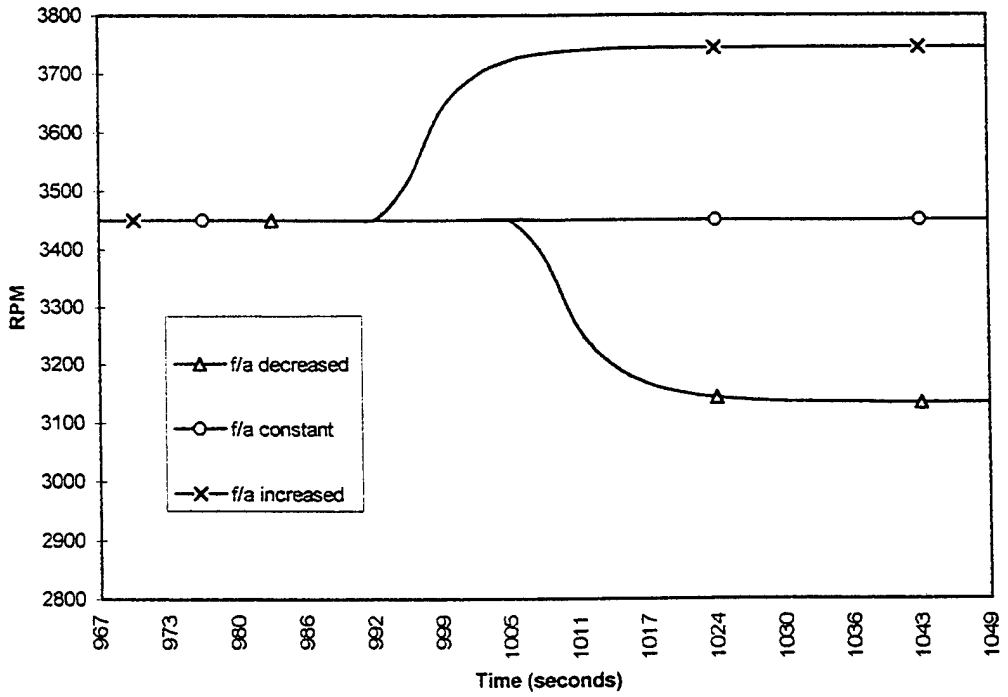

Figure 10. Influence of changes in fuel-air ratio during steady-state operations.

Figure 11 shows the effect of closing the air inlet guide vanes (IGVs) to the compressor. At steady-state conditions, the IGVs are 100% open, allowing the system to ramp-up to its reference mass flow rate (338.7 kg/s). In Figure 11, the "constant" line shows the IGVs remaining at 100% open. The other two lines represent, as noted, IGVs closed to 50% and completely closed (0%). The plot shows that the effect of closing the IGVs is reduced mass flow through the compressor, hence, less power output of the system.

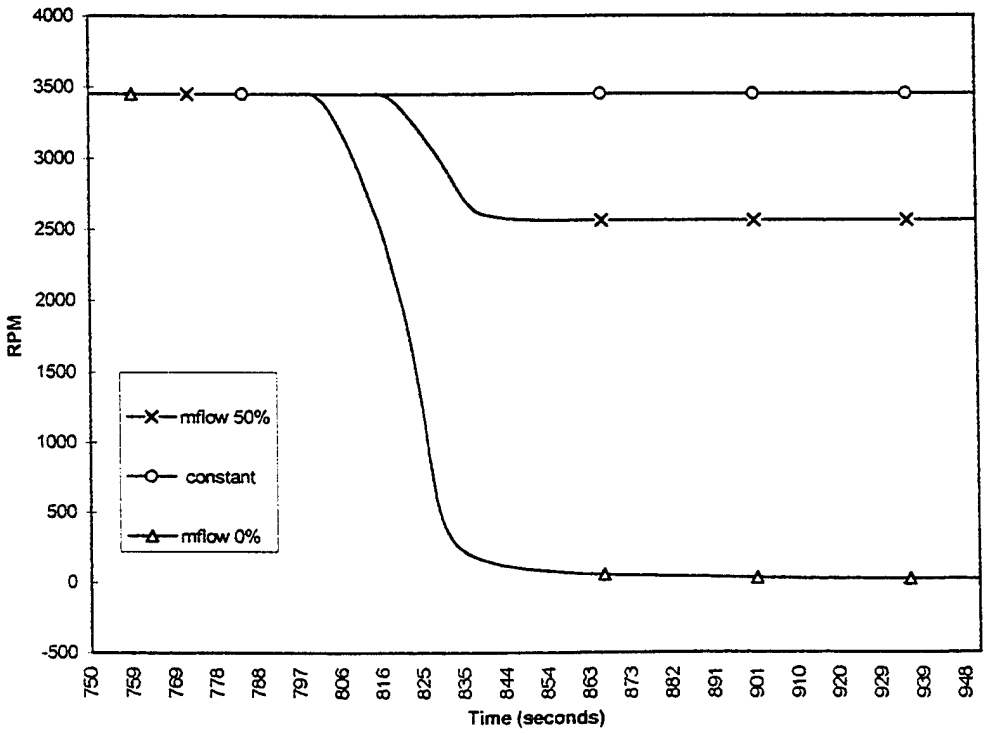

Figure 11. Influence of changes in mass flow (closing inlet guide vanes) during steady-state operations

Start-Up Routine

Start-up procedures of an actual industrial gas turbine system are given in [12]. These procedures are facilitated using an automatic control system and an external "start-up" device such as a diesel engine or an electric motor. Despite the lack of a control system, an investigation was done on gtsim1.vsm to see if these start-up procedures could be simulated.

To facilitate this test, a "start-up" engine was simulated by changing the sign of the load term in equation (1), making it negative. The mass flow rate and fuel input were set to zero. Using a VisSim ® "slider" block, the load was manually varied from a more negative value to a less negative value, allowing the system to come to 100% of design (reference state) rotational speed. Figure 12 was generated from this run:

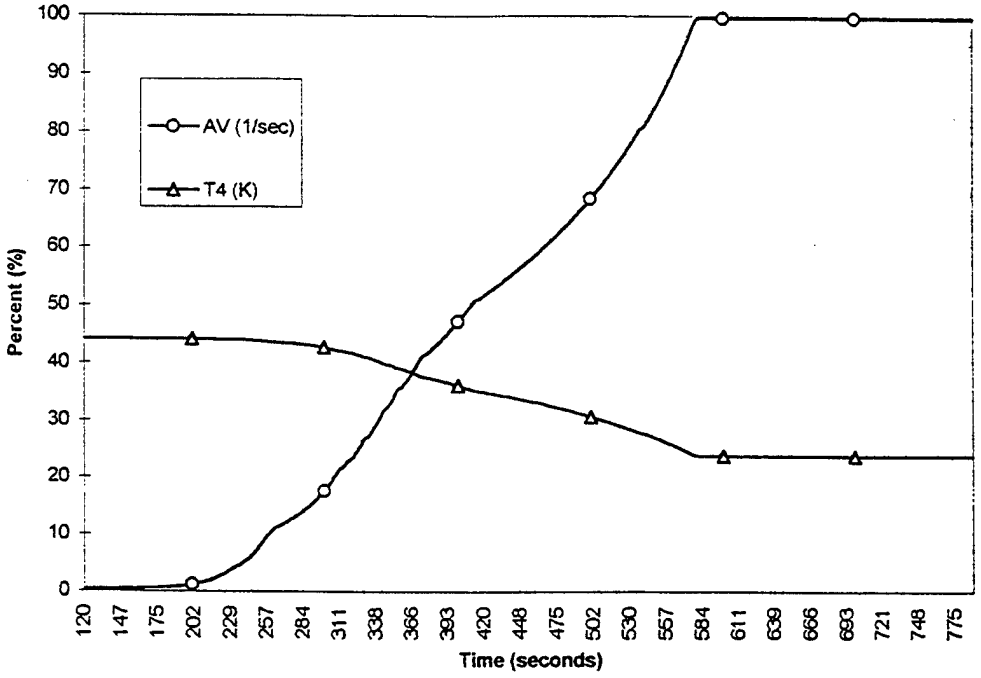

Figure 12. Trial run of start-up procedures given in reference [12].

The plot of T_4 does not match reference [12] due to the lack of fuel input during this run. In reference [12], there was fuel input, giving the system outlet temperate higher values than in Figure 12. This start-up trial of gtsim1.vsm did not exactly simulate reference [12]; however, it does demonstrate that this model can be adapted to an external start-up device and control system to simulate that in reference [12] or others.

CONCLUSIONS

A mathematical and computer model was developed to investigate the dynamic response of a simple (no reheat, regeneration, or other auxiliary equipment) single-shaft gas turbine system. The model used parameters normally incorporated in gas turbine design as well as compressor and turbine stage geometries and compressor and turbine material properties. Also incorporated was a combustion chamber model. Input parameters were included to enable the model to be adaptable to various system sizes and environments.

The results of several trials were displayed, showing how given parameters (e.g. fuel-air ratio, load, and efficiencies) were varied and results were compared. A thermodynamic balance of the adopted baseline state resulted in a 26% system thermal efficiency. Further, a literature search showed that industrial gas turbines are brought on-line from "cold" conditions via an elaborate start-up procedure. The goal of this procedure is dual: to avoid undue thermal stresses leading to fatigue, and to allow ready synchronization to external loads. The turbine model presented in this paper can respond to similar requirements as imposed manually by the programmer. In an uncontrolled start-up, the turbine does converge quite rapidly to steady-state

conditions. It is noteworthy that the peak temperature increases gradually at first, and more rapidly after the air flow is established. Most of the temperature increase is quite gradual, on the order of 50K/min.

Examination of the results from the trial runs show the computer model, gtsim1.vsm, as a functional gas turbine model, given the fact that no control system was incorporated. For a frictional load and constant fuel/air ratio, the turbine model converges to a steady-state condition. In this condition, the turbine and internal and external loads are in balance. Small departures of load and fuel/air ratio from steady-state values result in small departures in rotational speed. Because of the approach used, the computer model is easily adaptable to further improvements and a control system.

REFERENCES

[1] Johnson, D., Miller, R. W., and Rowen, W. I., *"Speedtronic ™ Mark V Gas Turbine Control System,"* General Electric Publication GER-3658C, 1993.

[2] Smith, D. L., and Stammetti, V. A., *"Comparative Controller Design for a Marine Gas Turbine Propulsion System,"* Journal of Engineering for Gas Turbines and Power, Vol. 112, April 1990.

[3] Smith, D. L., *"Linear Modeling of a Marine Gas Turbine Power Plant,"* ASME Paper 88-GT-71, 1988.

[4] Smith, D. L. and Stammetti, V. A., *"Sequential Linearization as an Approach to Real-Time Marine Gas Turbine Simulation,"* Journal of Engineering for Gas Turbines and Power, Vol. 112, April 1990.

[5] Ahluwalia, K. S., and Domenichini, R., *"Dynamic Modeling of a Combined-Cycle Plant,"* Journal of Engineering for Gas Turbines and Power, Vol. 112, April 1990.

[6] Hussain, A., and Seifi, H., *"Dynamic Modeling of a Single Shaft Gas Turbine,"* IFAC Symposium on Control of Power Plants and Power Systems, March 9-11, 1992.

[7] Facchini, B., *"A Simplified Approach to Off-Design Performance Evaluation of Single Shaft Heavy Duty Gas Turbines,"* ASME International Gas Turbine Institute Proceedings, Vol. 8, September 1993.

[8] Bettocchi, R., Spina, P. R., and Fabbri, F., *"Dynamic Modeling of Single-Shaft Industrial Gas Turbine,"* ASME Paper 96-GT-332, June 1996.

[9] Hattori, T., Ohnishi, H., and Taneda, M., *"Optimum Design Technique for Rotating Wheels,"* Journal of Engineering for Gas Turbines and Power, Vol. 110, January 1988.

[10] Bathie, W. W., *"Fundamentals of Gas Turbines,"* 2nd Ed., John Wiley & Sons, Inc., 1996.

[11] Cohen, H., Rogers, G. F. C., and Saravanamuttoo, H. I. H., *"Gas Turbine Theory,"* 3rd Ed., John Wiley & Sons, Inc., 1987.

[12] Rowen, W. I., *"Operating Characteristics of Heavy-Duty Gas Turbines in Utility Service,"* ASME Paper 88-GT-150, 1988.

[13] Operator's Manual, VisSim ® Software v. 2.0, Visual Solutions, Inc., 1995.

[14] Turbomachinery International Handbook/1995, Turbomachinery Publications, 1995.

APPENDIX A

Reference State Parameters

Compressor Variables

Material Density	7000 kg/m^3
Blade Height	0.41 m
Blade Length	0.02 m
Blade Thickness	0.004 m
Disk Radius	0.52 m
Disk Thickness	0.02 m
Number of Blades	62
Decrease Factor (of successive stage sizes)	0.98
Polytropic Efficiency	0.85

Turbine Variables

Material Density	7000 kg/m^3
Material Specific Heat	582 J/kgK
Blade Height	0.5 m
Blade Length	0.02 m
Blade Thickness	0.004 m
Disk Radius	0.4 m
Disk Thickness	0.02 m
Number of Blades	87
Decrease Factor (of successive stage sizes)	1.1
Polytropic Efficiency	0.89

Combustor Variables

Combustor Diameter	0.35 m
Combustor Length	0.7 m
Number of Combustors	8
Combustor Wall Thickness	0.008 m
Combustor Material Density	4510 kg/m^3
Combustor Material Specific Heat	582 J/kgK
Pressure Drop	2%

Thermodynamic Variables

Input Pressure	101325 Pa
Input Temperature	289 K
Ratio of Specific Heats for air	1.4
Ratio of Specific Heats for combustion mixture	1.33
Universal Gas Constant	8314 J/molK
Specific Heat of Air	1005 J/kgK
Specific Heat of Combustion Mixture	1100 J/kgK
Lower Heating Value of Fuel	50000000 J/kg
Molecular Weight of Air	28.85 kg/kmole

Other Variables

External Load Factor	2.0 kgm^2
Load Coefficient (Compressor)	0.3
Flow Coefficient (Compressor and Turbine)	0.72
Hub-to-Tip Ratio (Compressor)	0.75
Friction Load Factor	0.2 kgm^2

Results of gtsim1.vsm using these reference parameters

Fuel-Air Ratio (input)	0.013
Initial RPM Condition on Integrator Block	30 RPM
Turbine Inlet Temperature	1265 K
Turbine Outlet Temperature	680 K
Rotational Velocity	3450 RPM
Pressure Ratio	17.4
Time to reach steady state	approx. 725 seconds
Mass Flow Rate	338.7 kg/s
Power Output	56.6 MW
Compressor Isentropic Efficiency	0.78
Turbine Isentropic Efficiency	0.93

Appendix B - Survey of Turbomachinery Handbook/1995 [14]

Company	Model	Shaft Speed (RPM)	Pressure Ratio	Turbine Inlet Temp (K)	Exhaust Temp (K)	Exhaust Flow (kg/s)
Mechanical Drive Turbines						
ABB	GT-35	3450	12.0	1123	649	92.0
European	RLM2500	3600	18.4	1501	797	69.0
European	RLM2500+	3600	21.0	1501	785	83.0
European	RLM5000	3600	25.4	1443	707	121.0
Kvaerner	LM2500-PE	3600	18.4	1086	801	68.0
Kvaerner	LM6000-PA	3600	29.6	1126	735	125.7
Electrical Generation Turbines						
ABB	GT26	3000	30.0	1508	893	543.0
ABB	GT24	3600	30.0	1508	883	376.0
ABB	GT13E2	3000	14.6	1373	797	532.0
ABB	GT13D	3000	11.9	1263	763	394.0
ABB	GT11N2	3600	15.0	1358	797	375.0
ABB	GT11N	3600	13.3	1300	778	317.0
Ansaldo	V84.2	3600	10.8	***	821	353.0
Ansaldo	V84.3	3600	16.1	***	823	433.0
Ansaldo	V94.2	3000	11.0	***	816	514.0
Ansaldo	V94.3	3000	16.1	***	823	624.0
Dresser	DR-63G	3600	29.6	1104	736	177.0
Mitsubishi	MW501	3600	14.0	***	794	365.0
Mitsubishi	MW701	3000	14.0	***	786	453.0
Mitsubishi	501F	3600	14.6	***	853	437.0
Mitsubishi	701F	3000	16.0	***	826	667.0
Mitsubishi	501G	3600	19.0	***	866	544.0
MTU	LM2500+	3600	23.0	***	799	83.0
MTU	LM2500+	3000	23.0	***	784	84.0
Siemens	V84.2	3600	11.0	***	817	360.0
Siemens	V84.3A	3600	16.6	***	835	454.0
Siemens	V94.2	3000	11.1	***	813	519.0
Siemens	V94.3A	3000	16.6	***	835	540.0
Marine Drive Turbines						
FiatAvio	LM2500	3600	19.2	1130	826	69.8
GEC	LM2500	3600	18.0	***	813	70.0
Kvaerner	LM2500	3600	18.4	1086	801	68.0
MAN	FT8	3600	19.8	***	1131	84.1
MTU	LM2500+	3600	23.0	***	799	83.0
Pratt & Wh	FT8	3600	18.7	***	716	78.1
Rolls Royce	WR21	3600	12.7	***	629	73.0
Turbo Power	FT8	3600	19.8	***	716	83.9
Average Values		3429	18.1	1294	801	286.5

	Shaft Speed (RPM)	Pressure Ratio	Turbine Inlet Temp (K)	Exhaust Temp (K)	Exhaust Flow (kg/s)